JOURNAL OF CATALYSIS 82, 45–55 (1983)

Solid Electrolyte-Aided Study of Propylene Oxidation on Polycrystalline Silver

MICHAEL STOUKIDES AND COSTAS G. VAYENAS[1]

Massachusetts Institute of Technology, Cambridge, Massachusetts 02139

Received August 6, 1982; revised January 28, 1983

The oxidation of propylene on porous polycrystalline Ag films supported on yttria-stabilized zirconia was studied in a CSTR at temperatures between 290 and 400°C and atmospheric total pressure. Steady state kinetic measurements were combined with simultaneous *in situ* monitoring of the chemical potential of oxygen adsorbed on the silver catalyst, using the technique of solid electrolyte potentiometry (SEP). The kinetic and potentiometric results are consistent with a Langmuir–Hinshelwood reaction model with two types of chemisorbed oxygen. The reaction network kinetics are studied thoroughly and compared with those obtained during oxidation of propylene oxide, ethylene, and ethylene oxide on the same catalytic surface.

INTRODUCTION

Silver is the only catalyst known to produce epoxides from the catalytic gas phase oxidation of ethylene and propylene. The selectivity to propylene oxide is low, typically less than 5–10% (*1, 2, 4*). Thus the major industrial processes currently used for propylene oxide formation are the propylene–chlorohydrin and the "oxirane" process (*1*). However, propylene oxide production by direct oxidation of propylene on silver would be financially preferable if high yield and selectivity to propylene oxide could be achieved (*1*). Therefore several investigators have studied the kinetics of direct propylene oxidation (*2–10*) and the promoting effect of various compounds, including chlorinated hydrocarbons, CaO and BaO (*2, 4*). However, the mechanism of the reaction and the reason for the low selectivity to propylene oxide are still not well understood. Furthermore, there is little agreement among previous investigators about the reaction network kinetics.

Kaliberdo *et al.* (*2–4*) studied the kinetics of propylene oxidation on silver and concluded that epoxidation and deep oxidation are mainly parallel rather than consecutive reaction pathways (*8*). This is corroborated by the work of Cant and Hall (*9*) who studied oxidation of deuterium-labeled ethylene and propylene as well as simultaneous oxidation of unlabeled olefins with the corresponding ^{14}C-labeled epoxides. They found that the low selectivity to propylene oxide is not primarily due to fast propylene oxide oxidation, since most of the CO_2 produced originates from direct propylene oxidation, and elegantly demonstrated that the higher reactivity of propylene than ethylene for deep oxidation is due to the presence of the methyl group. Several interesting similarities between ethylene and propylene epoxidation over supported and unsupported silver have been uncovered by the work of Imachi *et al.* (*5*).

There is considerable evidence for the existence of surface deposits on Ag catalysts during reaction (*6, 10*). Frericks *et al.* (*10*) reported formation of a carbon-rich deposit on the Ag surface and proposed that the low selectivity to propylene oxide is caused by intermediate formation of acrolein which polymerizes and gets deeply oxidized to CO_2 and H_2O by gaseous oxygen. Kobayashi used a transient microreactor technique and found also strong evidence for the presence of a stable intermediate with C:H ratio of 1:2, which produces

[1] To whom all correspondence should be addressed: Dept. of Chemical Engineering, University of Patras, Patras, Greece

0021-9517/83 $3.00

CO_2 and H_2O (*6*). Some additional indirect evidence about the presence of carbon-rich polymeric residues on the silver surface during reaction was found in a recent study of propylene oxide oxidation on polycrystalline silver films (*11*). It was found that over a wide range of conditions, propylene oxide oxidation on silver is an oscillatory reaction. The rate and surface oxygen activity oscillations were attributed to periodic formation and combustion of surface polymeric residues (*11, 16*). In the same communication (*11*) the steady-state kinetics of the secondary propylene oxide oxidation on polycrystalline silver films were measured over a wide range of experimental conditions.

In the present communication we complete the kinetic investigation of the propylene oxidation network on silver by focusing on propylene epoxidation and deep oxidation over the same catalyst surfaces used for the study of propylene oxide oxidation (*11*). To gain additional information the kinetic studies were combined with simultaneous *in situ* measurement of the thermodynamic activity of oxygen on the silver surface, using the technique of solid electrolyte potentiometry (SEP) (*11, 14*). The results of the present investigation are then compared with those obtained during oxidation of ethylene on the same surfaces under similar gas composition, pressure, and temperature conditions (*12, 13*) in order to identify some of the similarities and differences in the kinetic behaviour of the two systems.

EXPERIMENTAL APPARATUS

Oxygen Activity Measurement

The reaction was studied in an oxygen concentration solid electrolyte cell with one Ag electrode serving as the catalyst under study. The apparatus and the reactor cell used have been described in detail in previous communications (*12, 13*). The total catalyst surface area was approximately 2000 cm^2. The catalyst preparation and characterization procedure was the same with that followed during the study of ethylene oxidation (*11, 12*). Auger spectroscopic analysis of the catalyst film before and after reaction has shown the surface to be fairly clean with only trace amounts of S, Cl, and Na impurities (*12*). Over the range of flow rates employed in the present study the reactor has been shown to behave as a CSTR (*12*).

Matheson certified standards of propylene diluted in nitrogen and zero-grade air were used as reactants. Both reactants could be further diluted in nitrogen in order to maintain the partial pressure of either oxygen or propylene constant. Gases were analyzed by means of a Perkin–Elmer gas chromatograph with a TC detector. A molecular sieve 5A column was used to separate O_2 and N_2 and a Porapak Q column was used to separate air, CO_2, propylene, and propylene oxide. A Beckman 864 IR CO_2 analyzer was used to monitor continuously the CO_2 concentration in the effluent stream. A J. Fluke differential voltmeter was used for the potentiometric studies.

The technique of solid electrolyte potentiometry (SEP) was used for oxygen activity measurement. SEP provides a continuous *in situ* measurement of the thermodynamic activity of oxygen adsorbed on the catalyst surface. It has been established (*12, 14*) that the measured open circuit emf reflects the difference in chemical potential of oxygen adsorbed on the two silver electrodes.

$$E = \frac{1}{4F}\left[\mu_{O_2}(\text{Ag catalyst}) - \mu_{O_2}(\text{Ag reference})\right] \quad (1)$$

The chemical potential of oxygen adsorbed on the reference electrode which is in contact with air ($P_{O_2} \sim 0.21$ bar) is given by

$$\mu_{O_2}(\text{Ag reference}) = \mu^{\circ}_{O_2}(g) + RT \ln (0.21) \quad (2)$$

where $\mu^{\circ}_{O_2}(g)$ is the standard chemical potential of oxygen at the temperature of interest. The activity a_0 of adsorbed oxygen can be defined by:

$$\mu_{O_2}(\text{catalyst}) = \mu^{\circ}_{O_2}(g) + RT \ln a_o^2 \quad (3)$$

Thus a_o^2 expresses the partial pressure of gaseous oxygen that would be in thermodynamic equilibrium with oxygen adsorbed on the catalyst surface, if such an equilibrium were established. Therefore, combining Eqs. (1), (2), and (3) one obtains:

$$a_o = (0.21)^{1/2} \exp \frac{2FE}{RT}. \quad (4)$$

The above equation is always valid, irrespective of whether thermodynamic equilibrium is established between gaseous and adsorbed oxygen. In the special case where thermodynamic equilibrium indeed exists between adsorbed and gaseous oxygen, then $a_o^2 = P_{O_2}$.

RESULTS

Kinetic Measurements

The catalytic oxidation of propylene was studied at temperatures between 290 and 420°C and atmospheric total pressure. The feed oxygen and propylene partial pressure were varied between 0.03–0.11 bar and 0.001–0.01 bars, respectively. Table 1 summarizes the kinetic and potentiometric data of this study.

The reaction network can be represented by the following scheme:

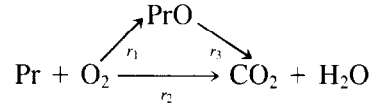

TABLE 1

Kinetic and Potentiometric Data for the Catalytic Oxidation of Propylene

Temp (°C)	Flow rate (cm^3 STP/min)	P_{Pr} (10^{-3} bar)	P_{O_2} (10^{-3} bar)	a_O	r_1 (10^{-6} mole/s)	r_2 (10^{-6} mole/s)
420	700	8.9	95	0.116	.08	1.76
420	700	5.56	98	0.142	.048	1.06
420	700	3.25	88	0.168	.031	0.643
420	700	1.85	93	0.204	.017	0.30
420	700	5.42	67	0.109	.046	1.03
420	700	5.7	47	0.083	.057	1.14
420	700	6.1	33	0.066	.054	1.07
375	700	9.3	95	0.053	.063	1.33
375	700	5.67	93	0.066	.039	0.90
375	700	3.07	88	0.090	.021	0.515
375	700	1.91	93	0.126	.015	0.28
375	700	6.0	69	0.045	.033	0.92
375	700	5.7	47	0.034	.028	0.92
375	700	6.0	30	0.0274	.032	0.90
330	500	8.5	95	0.014	.032	1.03
330	500	6.3	95	0.022	.028	0.78
330	500	3.2	86	0.073	.018	0.44
330	500	5.8	59	0.012	.020	0.78
330	500	6.5	40	0.008	.025	0.68
330	500	6.1	23	0.0074	.022	0.73
330	500	2.4	88	0.044	.010	0.30
290	360	9.1	110	0.0078	.011	0.60
290	360	5.4	102	0.0090	.008	0.45
290	360	3.4	113	0.0151	.007	0.31
290	360	1.9	112	0.0186	.005	0.22
290	360	5.6	62	0.007	.015	0.42
290	360	6.0	35	0.0055	.009	0.40
290	360	6.4	20	0.0037	.011	0.41

The three reaction rates r_1, r_2 (moles C_3H_6/s), and r_3 (moles C_3H_6O/s) are calculated as follows from the raw kinetic data of the CSTR: First r_3 is calculated using the partial pressure of propylene oxide P_{Pro} in the products and the rate expression obtained in the previous work on the same catalyst (*11*):

$$r_3 = K_3 \frac{K_{Pro}P_{Pro}}{1 + K_{Pro}P_{Pro}} \tag{5}$$

with

$$K_3 = 6.4 \exp\left(\frac{-19000}{RT}\right) \frac{\text{mole}}{\text{s}} \tag{6}$$

and

$$K_{Pro} = 0.010 \exp\left(\frac{10400}{RT}\right) \text{bar}^{-1}. \tag{7}$$

The rate of proplyene oxide oxidation r_3 was very small compared to r_2 ($r_3 \sim 0.001\ r_2$), thus essentially all CO_2 found in the products was produced from the direct propylene combustion. Unlike ethylene oxidation, the epoxidation rate was much smaller than the direct CO_2 formation as shown in Table 1.

Taking into account that the reactor is a CSTR, the reaction rates r_1, r_2 are calculated from the appropriate mass balances:

$$r_1 - r_3 = G\,X_{PrO} \tag{8}$$

$$r_2 + r_3 \approx r_2 = \tfrac{1}{3}G\,X_{CO_2} \tag{9}$$

where X_{PrO}, X_{CO_2} are the exit mole fractions of propylene oxide and CO_2 and G is the total molar flow rate. The values of r_1 and r_2 were also found to satisfy within 2% the mass balance requirement

$$r_1 + r_2 = G[X_{Pr,IN} - X_{Pr,OUT}], \tag{10}$$

where $X_{Pr,IN}$, $X_{Pr,OUT}$ are mole fractions of propylene in the feed and effluent stream, respectively. Volume changes were calculated to be negligible due to the high partial pressure of diluent N_2 (>80%).

The rate of propylene oxide formation r_1 is plotted in Fig. 1 versus the partial pressure of oxygen P_{O_2} for constant P_{Pr}. The rate of deep propylene oxidation r_2 is plotted versus P_{O_2} in Fig. 2. Similarly to ethylene oxidation, both r_1 and r_2 are essentially independent of the partial pressure of oxygen over the range of fuel lean gas compositions examined.

Figures 3 and 4 show the dependence of r_1 and r_2 versus P_{Pr} for different temperatures. It can be seen that at high temperatures both rates are first order in propylene but at lower temperatures the apparent reaction order tends to decrease.

It was found that all the kinetic data could be expressed rather accurately by the

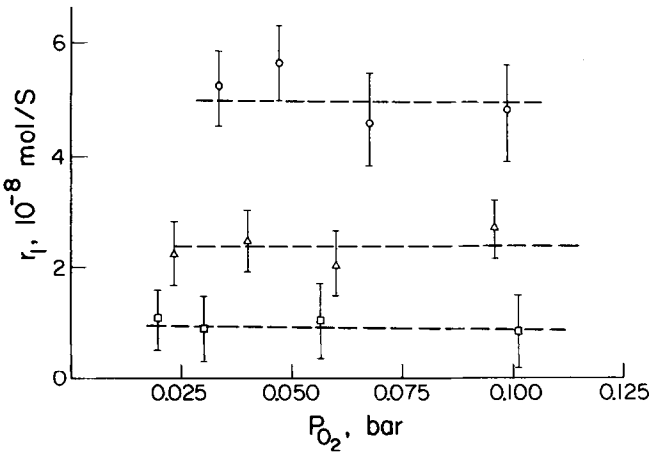

FIG. 1. Rate of propylene epoxidation versus P_{O_2}. □, 290°C. △, 330°C. ○, 420°C; $P_{Pr} = 6 \times 10^{-3}$ bar.

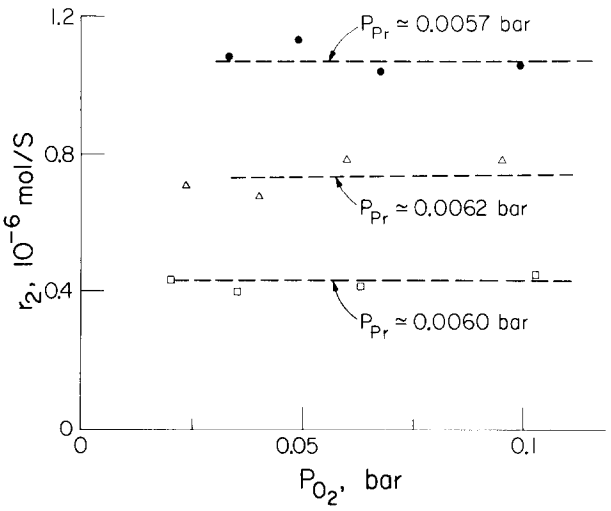

FIG. 2. Rate of direct propylene oxidation to CO_2 versus P_{O_2}. □, T = 290°C. △, T = 330°C. ○, T = 375°C; $P_{Pr} \approx 6 \times 10^{-3}$ bar.

rate expressions:

$$r_1 = K_1 \frac{K_{Pr}P_{Pr}}{1 + K_{Pr}P_{Pr}} \qquad (11)$$

$$r_2 = K_2 \frac{K_{Pr}P_{Pr}}{1 + K_{Pr}P_{Pr}} \qquad (12)$$

with

$$K_1 = 11.9 \exp\left(\frac{-22000}{RT}\right) \qquad (13)$$

$$K_2 = 32.9 \exp\left(\frac{-19000}{RT}\right) \qquad (14)$$

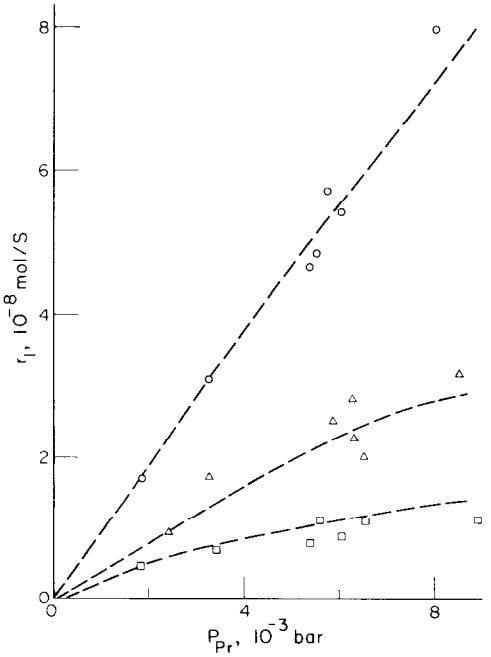

FIG. 3. Rate of propylene epoxidation versus P_{Pr} at 290°C (□), 330°C (△); and 420°C (○).

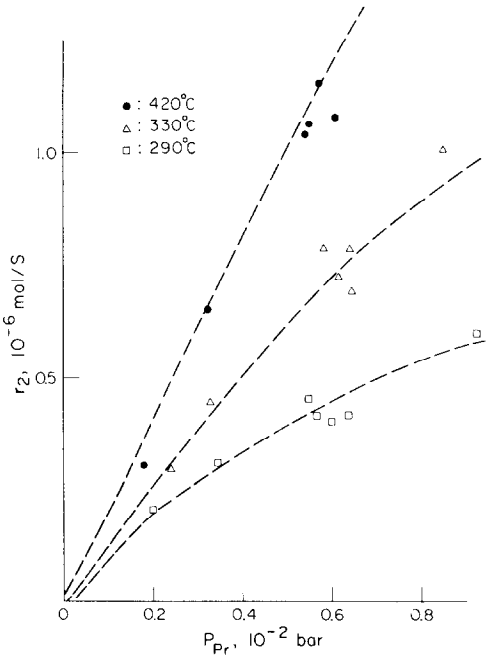

FIG. 4. Rate of direct propylene oxidation to CO_2 versus P_{Pr}.

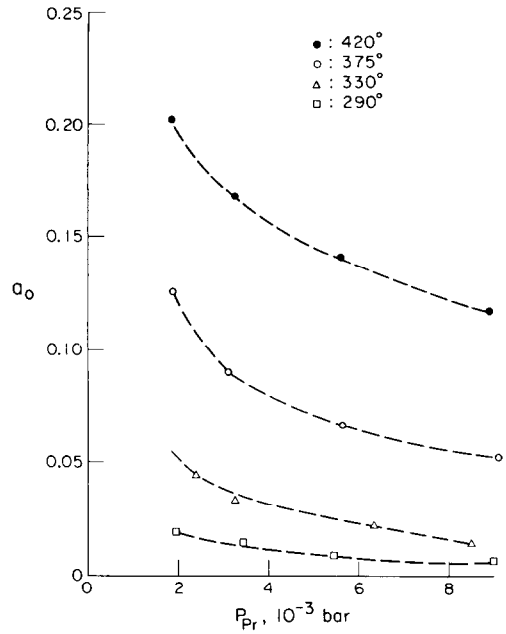

FIG. 5. Oxygen activity dependence on P_{Pr} at constant $P_{O_2} = 9.5 \times 10^{-2}$ bar.

$$K_{Pr} = 1.2 \times 10^{-4} \exp\left(\frac{15{,}000}{RT}\right). \quad (15)$$

These equations are formally similar to those obtained during ethylene oxidation, on the same catalyst.

Oxygen Activity Measurements

Similarly to ethylene, ethylene oxide, and propylene oxide oxidation, it was found that in general during propylene oxidation $a_o^2 < P_{O_2}$, i.e., thermodynamic equilibrium is not established between adsorbed oxygen and oxygen in the gas phase. The dependence of the surface oxygen activity a_O on the partial pressure of propylene for constant P_{O_2} is shown in Fig. 5. In Fig. 6 a_o is plotted versus P_{O_2} for constant P_{Pr}. From these figures it can be seen that:

(a) a_O increases with increasing P_{O_2} at constant temperature and P_{Pr}.

(b) a_O decreases with increasing P_{Pr} at constant temperature and P_{O_2}.

(c) a_O increases with increasing temperature at constant gas composition.

Several functional forms were examined in order to describe the dependence of a_O on gas-phase composition. It was found that all the a_O measurements could be correlated rather accurately by:

$$\frac{a_O}{P_O^{1/2} - a_O} = KP_{Pr}^{-1} + K' \quad (16)$$

with

$$K = 22{,}800 \exp\left(\frac{-21{,}500}{RT}\right).$$

This is shown in Figs. 7 and 8.

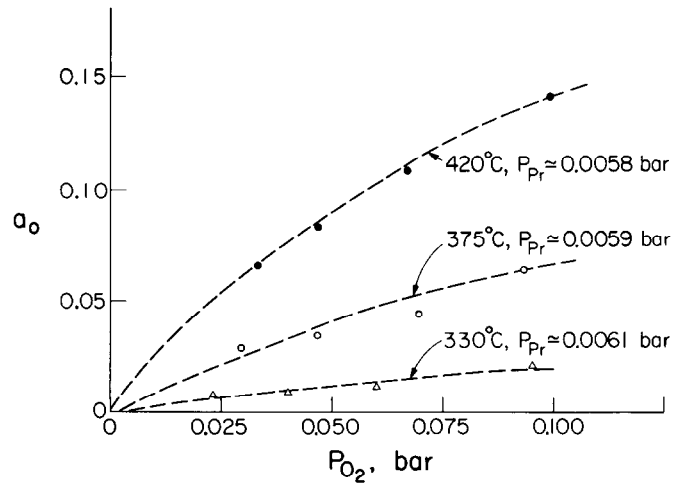

FIG. 6. Oxygen activity versus P_{O_2}.

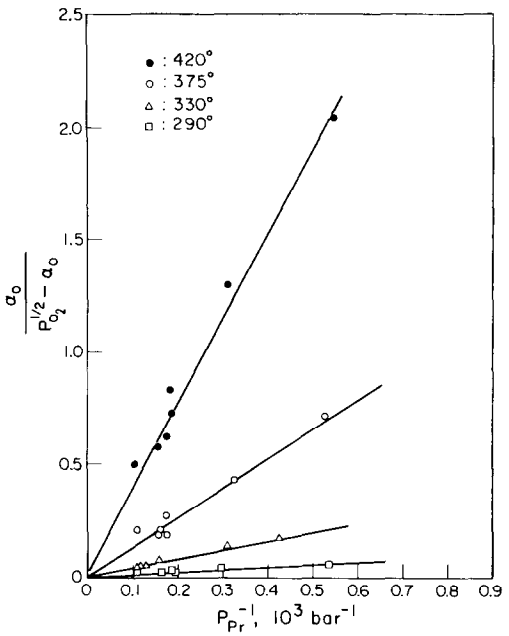

FIG. 7. Oxygen activity dependence on gas composition and temperature.

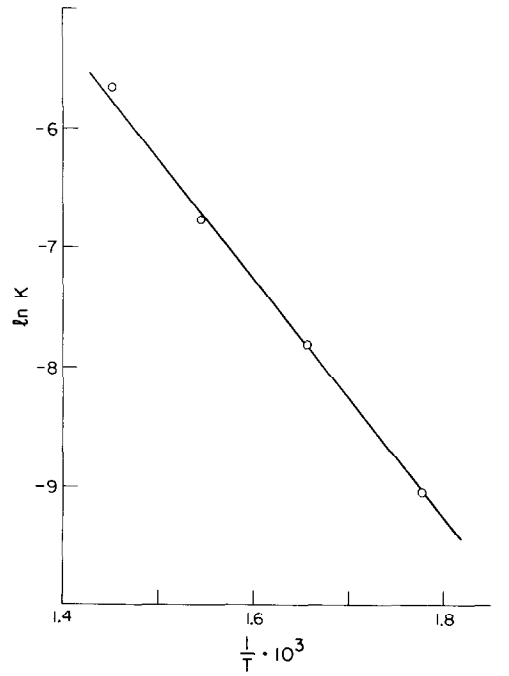

FIG. 8. Temperature dependence of the parameter K.

DISCUSSION

A satisfactory kinetic model for propylene oxidation should account not only for the kinetics (Eqs. (11) and (12)) but also for the surface oxygen activity behaviour (Eq. (16)). Such a model is presented below.

In agreement with previous studies (*12, 13*) we assumed the existence of two types of adsorbed oxygen, i.e., molecular and atomic. Molecular oxygen is assumed to yield propylene oxide and to adsorb on surface sites S_3, while atomic oxygen adsorbs on S_2 sites. Propylene and propylene oxide adsorb on S_1 sites on the silver surface. We assume Langmuir-type adsorption for propylene and thermodynamic equilibrium between surface and gaseous propylene. It thus follows that the coverage θ_{Pr} of propylene on S_1 sites is given by

$$\theta_{Pr} = K_{Pr}P_{Pr}/(1 + K_{Pr}P_{Pr}), \qquad (17)$$

where K_{Pr} is the adsorption coefficient of propylene, provided P_{PrO} is small enough so that $K_{Pr}P_{Pr} \gg K_{PrO}P_{Pro}$ ($\theta_{Pro} \ll \theta_{Pr}$).

Similarly, assuming Langmuir-type adsorption for molecular oxygen on S_3 sites and thermodynamic equilibrium between molecularly adsorbed and gaseous O_2 one obtains

$$\theta_{O_2} = K_{O_2}P_{O_2}/(1 + K_{O_2}P_{O_2}),$$

where θ_{O_2} is the molecular oxygen coverage and K_{O_2} is the molecular adsorption coefficient of oxygen. Assuming that the electrochemically measured surface oxygen activity represents atomically adsorbed oxygen (*13*), the coverage θ_O of atomic oxygen adsorbed is given by:

$$\theta_O = K_O a_O/(1 + K_O a_O) \qquad (18)$$

which relates two intrinsic surface properties and is valid irrespective of whether thermodynamic equilibrium is established between gaseous and atomically adsorbed oxygen (*13*).

On the basis of the above assumptions it follows that the rate of propylene oxide for-

mation r_1 is given by:

$$r_1 = K_1\theta_{Pr}\theta_{O_2} = K_1 \frac{K_{Pr}P_{Pr}}{1 + K_{Pr}P_{Pr}} \cdot \frac{K_{O_2}P_{O_2}}{1 + K_{O_2}P_{O_2}} \quad (19)$$

which reduces to the experimental rate expression if $K_{O_2}P_{O_2} \gg 1$. This is quite reasonable since excess oxygen was used in all the experiments. However, Eq. (19) can also explain the first-order dependence on O_2 and zero-order dependence in propylene observed by Vaabel *et al.* (8) with fuel-rich mixtures. Similarly the rate of propylene deep oxidation to CO_2 is given by:

$$r_2 = K_2\theta_{Pr}\theta_O = K_2 \frac{K_{Pr}P_{Pr}}{1 + K_{Pr}P_{Pr}} \cdot \frac{K_O a_O}{1 + K_O a_O} \quad (20)$$

which reduces to the experimental expression (11) if $K_O a_O \gg 1$.

From Eqs. (17) and (18) it follows that the experimentally determined parameter K_{Pr} can be interpreted as the adsorption coefficient of propylene on silver. According to Eq. (15) it follows that the enthalpy and entropy of adsorption of propylene on silver are

$$\Delta H_{Pr} = -15 \text{ Kcal/mole}$$

$$\Delta S_{Pr} = -17.9 \text{ cal/mole} \cdot {}^\circ\text{K}.$$

The surface oxygen activity dependence on temperature and gas-phase composition can be explained by considering a steady-state mass balance for absorbed atomic oxygen:

$$K_{ad}P_{O_2}^{1/2}(1 - \theta_O) = K_d\theta_O - K_2\theta_{Pr}\theta_O. \quad (21)$$

The left-hand side term corresponds to atomic oxygen adsorption and the right-hand side terms correspond to atomic oxygen desorption and surface reaction, respectively. In the absence of propylene Eq. (21) reduces to the usual Langmuir isotherm with $K_O = \frac{K_{ad}}{K_d}$. Experimental justification for the first-order adsorption and desorption terms has been provided in previous communications (*12, 13*). Dividing Eq. (21) by $K_{ad}(1 - \theta_O)$ one obtains:

$$P_{O_2}^{1/2} - \frac{K_d}{K_{ad}} \cdot \frac{\theta_O}{(1 - \theta_O)} = \frac{K_2}{K_{ad}}\theta_{Pr}\frac{\theta_O}{(1 - \theta_O)}. \quad (22)$$

Taking into account Eq. (16) one can rewrite Eq. (22) in the form

$$P_{O_2}^{1/2} - a_O = \frac{K_2}{K_d}\theta_{Pr}a_O. \quad (23)$$

Using Eq. (17) and taking the reciprocal of both terms one obtains:

$$\frac{a_O}{P_{O_2}^{1/2} - a_O} = \frac{K_d}{K_2} + \frac{K_d}{K_2K_{Pr}}\frac{1}{P_{Pr}} \quad (24)$$

which is the experimental Eq. (16) with

$$K = \frac{K_d}{K_2K_{Pr}}$$

and

$$K' = \frac{K_d}{K_2}. \quad (25)$$

Furthermore, from the experimental values of K, K_2, K_{Pr} (Eqs. (16), (14), (15)) one can calculate K_d, the desorption coefficient of atomic oxygen:

$$K_d = 89.5 \exp\left(\frac{-25{,}500}{RT}\right) \text{ g atom O/s}. \quad (26)$$

The activation energy for atomic oxygen desorption found here (25.5 Kcal/mole) is in good agreement both with values reported by previous workers (*15, 17*) and also with the values extracted from similar SEP-aided studies of ethylene oxide (*12*) and propylene oxide oxidation (*11*) (Table 3).

Aside from an apparent compensation effect, the preexponential values of K_d obtained in these three studies are also in reasonable agreement (Table 3). This provides additional support for the proposed interpretation of the kinetic and potentiometric results.

The kinetic expressions obtained in this study (Eqs. (11)–(15)) show conclusively that the low selectivity to propylene oxide,

TABLE 2

Comparison of the Reactivities of Propylene and Ethylene Oxidations

Rate expression	a_O expression	Kinetic constants (molecules fuel/surface Ag atom · s)	Adsorption coefficients (bar^{-1})	Typical turnover number value (300°C, $P_i = 10^{-2}$ bar)	Remarks
		Propylene Oxidation		(molecules fuel/surface Ag atom · s)	
$r_1 = \frac{K_1 K_{Pr} P_{Pr}}{1 + K_{Pr} P_{Pr}}$	$\frac{P_{O_2}^{1/2}}{a_O} - 1 = K_A P_{Pr}^{-1} + K'_A$	$K_1 = 2.9 \times 10^6 \exp(-11000/T)$	$K_{Pr} = 1.2 \times 10^{-4} \exp(7500/T)$	$r_1 = 4.7 \times 10^{-3}$	
$r_2 = \frac{K_2 K_{Pr} P_{Pr}}{1 + K_{Pr} P_{Pr}}$		$K_2 = 8.3 \times 10^6 \exp(-9500/T)$		$r_2 = 0.18$	
$r_3 = \frac{K_3 K_{Pro} P_{Pro}}{1 + K_{Pro} P_{Pro}}$	$\frac{P_{O_2}^{1/2}}{a_O} - 1 = K_B P_{Pro}^{-1} + K'_B$	$K_3 = 1.6 \times 10^6 \exp(-9500/T)$	$K_{Pro} = 10^{-2} \exp(5250/T)$	$r_3 = 4.2 \times 10^{-2}$ $r_3^* = 3.2 \times 10^{-4}$	Rate and emf oscillations
		Ethylene Oxidation			
$r'_1 = \frac{K'_1 K_{ET} P_{ET}}{1 + K_{ET} P_{ET}}$	$\frac{P_{O_2}^{1/2}}{a_O} - 1 = K_C \frac{P_{ET}}{P_{O_2}}$	$K'_1 = 7 \times 10^4 \exp(-7300/T)$	$K_{ET} = 8.7 \times 10^{-4} \exp(5800/T)$	$r'_1 = 4.3 \times 10^{-2}$	
$r'_2 = \frac{K'_2 K_{ET} P_{ET}}{1 + K_{ET} P_{ET}}$		$K'_2 = 5 \times 10^7 \exp(-11100/T)$		$r'_2 = 2.3 \times 10^{-2}$	
$r'_3 = \frac{K'_3 (K_{ETO} P_{ETO})^2}{1 + (K_{ETO} P_{ETO})^2}$	$\frac{P_{O_2}^{1/2}}{a_O} - 1 = K_D P_{ETO}^2$	$K'_3 = 3.6 \times 10^6 \exp(-10200/T)$	$K_{ETO} = 5.7 \times 10^{-3} \exp(5300/T)$	$r'_3 = 1.4 \times 10^{-2}$ $r'^*_3 = 2.5 \times 10^{-5}$	

(typically less than 5%, as shown in Table 1), is due primarily to the very fast direct propylene oxidation and the corresponding slow rate of epoxidation (Table 2) and not very much due to the reactivity of propylene oxide for further oxidation. Thus typically more than 98% of the CO_2 produced comes from direct propylene oxidation, since r_2 was 2 to 3 orders of magnitude larger than r_3^* during the runs, although the intrinsic reactivities of propylene and propylene oxide for deep oxidation are comparable (Table 2). This is because very little epoxide was produced due to the low value of r_1. It should be noted, however, that even if r_2 could be somehow totally suppressed, silver still would not be a satisfactory commercial catalyst for propylene oxidation, since the intrinsic rate of epoxidation r_1 would be 1 order of magnitude slower than the rate of propylene oxide deep oxidation r_3.

Although self-sustained rate oscillations were observed during propylene oxide oxidation (*11*), only steady-state behaviour was observed during propylene oxidation on the same silver surface. This is not surprising since the amplitude of the rate oscillations was typically 2–15% of r_3 (*11*), and r_3 amounted to less than 2% of the rate of CO_2 production during the present investigation. Thus the expected fluctuations in the total rate of CO_2 production are of order 0.1%, i.e., below the sensitivity limit of the ir analyzer used for the reactor effluent stream analysis. We note that ethylene and ethylene oxide oxidation on the same surface did not give rise to oscillations, which corroborates the proposition that rate oscillations during propylene oxide oxidation on silver are caused by the peculiarities of propylene oxide chemisorption on silver, i.e., formation of relatively stable polymeric residues on the catalyst surface (*11*). Evidence for the existence of such polymeric residues on silver surfaces during propylene oxidation has been found by Kobayashi who used a transient response method to study propylene oxidation on silver oxide catalysts containing sodium chloride and sodium hydrogen sulfate at temperatures between 150 and 175°C (*6*).

Table 3 summarizes the kinetic and potentiometric results of the present investigation and compares them with previous studies of the oxidation of propylene oxide (*11*), ethylene (*13*), and ethylene oxide (*12*) on the same catalyst surface. The reactive oxygen uptake (*12*) of the polycrystalline Ag film used in all these studies was 2×10^{-6} mole O_2 and in extracting the turnover rates and turnover rate constants of Table 2 we have assumed a 1 : 1 stoichiometry between surface silver atoms and chemisorbed oxygen atoms. This assumption is arbitrary but can cause only a systematic error which does not affect the comparison of the turnover numbers. The turnover rates r_1, r_2, and r_3 for the propylene oxidation system and the corresponding ones for ethylene oxidation, i.e., r_1', r_2', r_3', have been all calculated at the same "standard" conditions, i.e., $T = 300$°C and $P_i = 0.01$ bar, where i represents propylene, ethylene, propylene oxide, or ethylene oxide. The rates of propylene oxide and ethylene oxide oxidation r_3^*, and $r_3'^*$, respectively have been also calculated under typical reactor operating conditions ($T = 300$°C, $\tau =$ 3 s, 0.01 bar propylene or ethylene pressure). It can be seen that r_3^*, and $r_3'^*$ are considerably smaller than r_1, r_2, r_1', and r_2'; therefore, in both cases the main pathway to CO_2 formation is direct olefin deep oxidation.

TABLE 3

Comparison of K_d Values Extracted from Kinetic and emf Data of Ethylene Oxide, Propylene Oxide, and Propylene Oxidation on a Ag Film with a Reactive Oxygen Uptake of 2×10^{-6} mole O_2

	K_d (s^{-1})	Ref.
Ethylene oxide oxidation	$3.6 \times 10^6 \exp(-10{,}200/T)$	(*12*)
Propylene oxide oxidation	$3.8 \times 10^7 \exp(-13{,}800/T)$	(*11*)
Propylene oxidation	$2.2 \times 10^7 \exp(-12{,}800/T)$	This work

Table 2 shows that one reason for the very low selectivity to epoxide during propylene oxidation in comparison with ethylene oxidation, is the higher reactivity of propylene for CO_2 formation, which is likely due to the presence of the methyl group (*9*). Another more important reason is the much higher rate of epoxidation during ethylene oxidation, which appears to be due to the considerably lower activation energy for ethylene oxide formation. This may be related to the lower heat of adsorption of ethylene, as indicated from the experimental values of the adsorption coefficients K_{ET} and K_{Pr}.

The potentiometric oxygen activity results during oxidation of propylene, propylene oxide, ethylene, and ethylene oxide are also shown in Table 2. the similarity of the functional form in these four experimentally derived relations is not accidental, since the term $P_{O_2}^{1/2}/a_O - 1$ represents the deviation from thermodynamic equilibrium between gaseous and adsorbed atomic oxygen. This deviation is due to the fact that the intrinsic rate of surface atomic oxygen formation, resulting from oxygen adsorption, is comparable to the intrinsic rate of the surface oxidation step (Refs. (*11–13*) and Eq. (21)).

In summary the results of the present steady-state kinetic and potentiometric investigation of propylene oxidation on silver films are consistent with a Langmuir–Hinshelwood reaction model with two types of adsorbed oxygen. The major source of CO_2 production is direct propylene oxidation, which is typically 30 times faster than the rate of epoxidation. The presence of propylene oxide in the reactor does not induce measurable oscillations in the rate of propylene epoxidation or deep oxidation which supports the proposition that rate oscillations during propylene oxide oxidation on silver are not due to an oxidation–reduction type mechanism but are related to the ability of propylene oxide to form relatively stable polymeric structures on the catalyst surface (*11*).

ACKNOWLEDGMENTS

This research was supported under NSF Grant CPE-8009436 and under a C.-H. Dreyfus Foundation Award Grant.

REFERENCES

1. *Chem. Eng. Progr.* **76**(1), 53 (1980).
2. Kaliberdo, L. M. *et al.*, *Kinet. Katal.* **8**(2), 463 (1967).
3. Kaliberdo, L. M., Vaabel, A. S., and Torgasheva, A. A., *Kinet. Katal.* **8**(1), 105 (1967).
4. Kaliberdo, L. M., and Zhukova, G. G., *Izv. Nauchno-Issled. Inst. Nefte-Uglekhim. Sint. Irkutsk. Univ.* **9**, 136 (1967).
5. Imachi, M., *et al.*, *J. Catal.* **70**, 177 (1981).
6. Kobayashi, M., *Canad. J. Chem. Eng.* **58**, 588 (1980).
7. Manara, G., and Parravano, G., *J. Catal.* **32**, 72 (1974).
8. Vaabel, A. S., *et al.*, *Kinet. Katal.* **9**(5), 1053 (1968).
9. Cant, N. W., and Hall, W. K., *J. Catal.* **52**, 81 (1978).
10. Frericks, I. C., Bouwman, R., and Geenen, P. V., *J. Catal.* **65**, 311 (1980).
11. Stoukides, M., and Vayenas, C. G., *J. Catal.* **74**, 266 (1982).
12. Stoukides, M., and Vayenas, C. G., *J. Catal.* **64**, 18 (1980).
13. Stoukides, M., and Vayenas, C. G., *J. Catal.* **69**, 18 (1981).
14. Wagner, C., *Adv. Catal.* **21**, 323 (1970).
15. Kilty, P. A., Rol, N. C., and Sachtler, W. M. H., Proceedings 5th International Congress on Catalysis, Miami, Fla. (J. W. Hightower, Ed.), Paper 64, p. 929, Amer. Elsevier, New York, 1972.
16. Stoukides, M., Seimanides, S., and Vayenas, C., *in* "Chemical Reaction Engineering-Boston" (J. Wei and C. Georgakis, Eds.), ACS Symp. Series 196, 165, 1982.
17. Czanderna, A. W., *J. Colloid Interface Sci.* **24**, 500 (1967).